

Superconductivity Transition Dependence of the Thermal Crosstalk in $\text{YBa}_2\text{Cu}_3\text{O}_{7-x}$ Edge-Transition Bolometer Arrays

Ali Bozbey, *Student Member, IEEE*, Mehdi Fardmanesh, *Senior Member, IEEE*, Juergen Schubert, and Marko Banzet

Abstract—The effect of the superconductivity transition on the thermal crosstalk in $\text{YBa}_2\text{Cu}_3\text{O}_{7-x}$ edge-transition bolometer arrays is investigated for DC to midrange modulation frequency infrared radiation. The bolometers in the arrays were designed with various distances on SrTiO_3 (100) substrates. We have observed a change in the thermal crosstalk between neighbor devices through the superconductivity transition temperature range. Superconductivity transition dependence of the thermal coupling between the devices was measured by utilizing the thermal conductance measurement methods developed for the bulk material. The knee points in the magnitude of the response versus modulation frequency curves of the devices were also determined by illuminating one of the bolometers in the arrays and measuring the response of the neighbor devices. By using the knee frequency and the distance between the bolometers, the modulation frequency criterion for crosstalk-free response at the transition region in various array structures is found and the results of the thermal coupling measurements are further studied and presented here.

Index Terms—Bolometer array, infrared detector, superconductivity, thermal conductivity, thermal crosstalk.

I. INTRODUCTION

STUDYING the crosstalk in $\text{YBa}_2\text{Cu}_3\text{O}_{7-x}$ (YBCO) edge transition bolometer arrays gives insights into the thermal diffusion process in the substrate material leading to design optimization for engineering applications. So far, there have been studies on the response of single device bolometers mostly for thermal modeling purposes [1]–[5], and recently on bolometer arrays [6], [7]. The phonon studies on high T_c superconductors and related substrate materials using infrared optical properties have been a major topic of the study as well [8]–[11]. For instance, Misochko *et al.* showed that the low-frequency phonon characteristics in the YBCO superconductor are strongly affected by the temperature [11]. To the best of our knowledge, a systematic study has not been reported that explains the physical reasons behind the observed crosstalk in YBCO bolometer arrays. By investigating the temperature

Manuscript received May 3, 2005; revised August 23, 2005. This paper was recommended by Associate Editor M. Mueck.

A. Bozbey is with the Electrical and Electronics Engineering Department, Bilkent University, Ankara 06800, Turkey (e-mail: bozbey@ieee.org).

M. Fardmanesh is with the Electrical and Electronics Engineering Department, Bilkent University, Ankara 06800, Turkey, and also with the Electrical Engineering Department, Sharif University of Technology, Tehran, Iran (e-mail: fardmanesh@ee.bilkent.edu.tr).

J. Schubert and M. Banzet are with the ISG1-IT and Center of Nanoelectronic Systems for Information Technology, Forschungszentrum Juelich GmbH, D-52425 Juelich, Germany.

Digital Object Identifier 10.1109/TASC.2005.861040

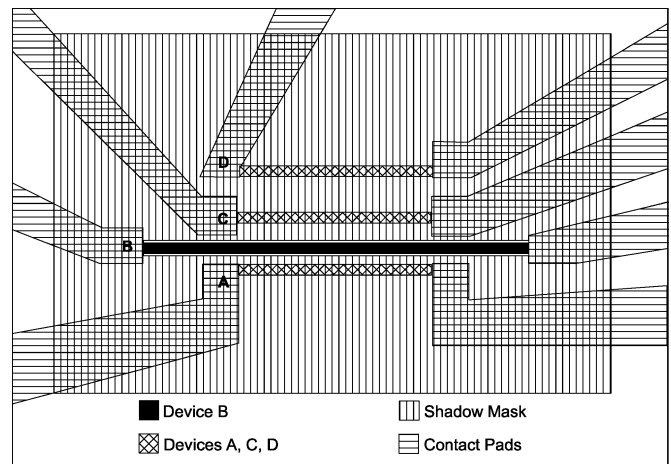


Fig. 1. Top view of the test devices. The illuminated device and the neighbor devices are shown together with the shadow mask.

dependence of the crosstalk between the devices in an array, we investigate the lateral heat diffusion process and phonon characteristics of the YBCO bolometers, particularly in their substrate material, that leads to optimal designs for engineering applications.

II. SAMPLES AND EXPERIMENTAL SETUP

We prepared 4×1 bolometer arrays in 200-nm-thick YBCO films deposited by pulsed laser deposition on crystalline substrates to investigate the thermal coupling or the crosstalk between the devices in the form of arrays of long bridges. The illuminated device in the array had an area of $20 \mu\text{m} \times 1 \text{mm}$ and the test neighbor devices had areas of $20 \mu\text{m} \times 0.75 \text{mm}$. In order to measure the crosstalk between the devices, it is essential to keep the test bolometers optically isolated from the environment. However, it was further taken into consideration that optically isolating the devices does not cause additional thermal coupling artifacts in the array. The four neighbor devices of our design are shown in Fig. 1. One bolometer, the “source device,” (named *B*) is illuminated with modulated infrared (IR) radiation whereas the remaining three bolometers, “sense devices,” are blocked with a free-standing reflecting mask. The separations of the sense bolometers, named *A*, *C*, and *D*, from the source bolometer were 40, 60, and $170 \mu\text{m}$, respectively.

The radiation blocking was achieved in a flip-chip configuration. The reflecting mask was made of a 250-nm-thick sputtered silver layer on 0.1-mm glass so that the IR transmittance was

negligible. Then using standard lithography process, a 25- μm -wide groove was opened in the reflecting layer. A 1.4- μm -thick photoresist layer was spun and a larger window was opened so that the mask was free standing on top of the devices, eliminating any parasitic thermal or electrical contacts that could affect the measurements. Finally, the groove was aligned and fixed on top of the source bolometer, as shown in Fig. 1. The contact paths and pads were coated by a sputtered gold layer so that the YBCO contact paths with nonzero resistance at the operating temperatures were shorted assuring that the generated response is only due to the bridges. The gold-deposited parts of the YBCO are shown in horizontal hatch pattern and the bridges are shown in cross hatch pattern in Fig. 1. The effective lengths of the bridges facing the direct thermal coupling were 0.5 mm, so that the lateral thermal conductance dominates over the longitudinal thermal conductance of the devices. The responses of the samples were measured using a DC bias current I_{bias} in four-probe configuration using an automated low noise characterization setup. The temperature of the substrate was controlled with a maximum 20 mK deviation from the target temperature using a liquid nitrogen dewar (Janis VPF-475) and a software PID controller. The phase and magnitude of the optical response of the devices were measured with SR 850 DSP lock-in amplifier, the input of which was amplified with an ultralow noise preamplifier (Stanford SR 570). As a radiation source, electrically modulated, fiber coupled IR laser diode with wavelength of 850 nm, and 12 mW power was used [4]. The system is capable of measuring all four devices in one cooling cycle without altering the electrical or thermal contacts, or the optical setup. In all the measurements, the magnitude of the response was at least one order of magnitude greater than the system noise.

The responses of the devices were measured versus radiation modulation frequency in the range of 1 Hz to 100 KHz, limited by the lock-in amplifier. During the measurements, the temperature was fixed at three different values. First, the temperature was fixed at the middle of the superconductivity transition where the highest response magnitude was obtained ($T_{c\text{-mid}}$), then it was fixed above and below the $T_{c\text{-mid}}$ to get a response magnitude approximately 10% of the maximum. These temperature values were defined as $T_{c\text{-onset}}$ and $T_{c\text{-zero}}$, respectively. For the reported sample, $T_{c\text{-zero}}$, $T_{c\text{-mid}}$, and $T_{c\text{-onset}}$ values were 89.2 K, 89.9 K, and 91.3 K, respectively.

III. RESULTS AND DISCUSSION

The voltage responses of the sense-devices versus the radiation modulation frequency shown in this study can be divided into two main parts: the response generated due to the crosstalk between the source-device and the response generated by the leaking laser beam directly due to the imperfect blocking of the radiation by the reflecting shadow mask. For example, the response of the device *D* in Fig. 2 is due to the crosstalk up to about 700 Hz and mainly due to the direct absorption of the leaking laser beam after about 2.5 kHz. As observed in Fig. 2, the phase and magnitude behavior of the response of device *D* are the same as the source device *B* for $f \geq 2.5$ kHz. For device *D*, which is separated by 170 μm distance, the crosstalk-free

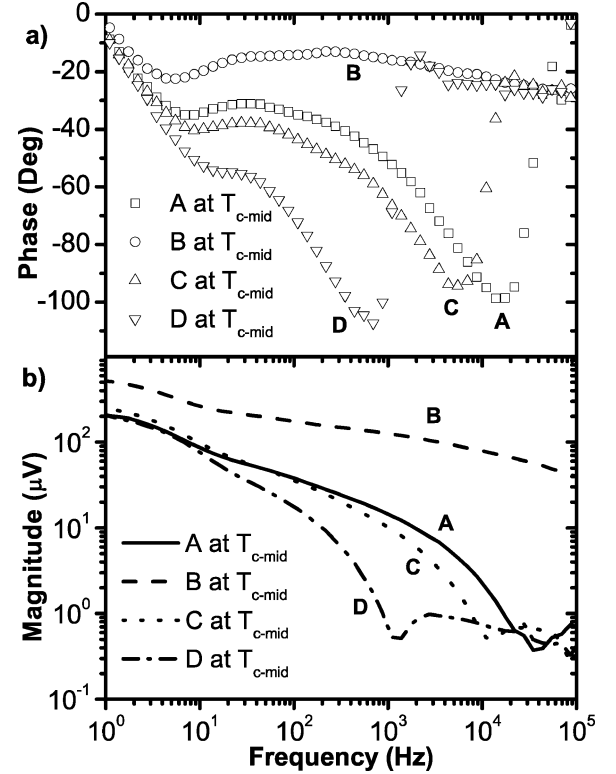


Fig. 2. (a) Phase and (b) magnitude of the IR response versus frequency of bolometers *A*, *B*, *C*, and *D* on 1-mm-thick SrTiO₃ substrate at $T_{c\text{-mid}}$. The effect of the separation distance on the response is clearly seen.

modulation frequency is around 1 kHz. Above this frequency, the coupling is expected to become negligible and the unblocked input laser line starts to dominate. As observed in Fig. 2(b), the magnitude of the response of device *D* at higher frequencies ($f \geq 10$ kHz) is approximately two orders smaller than that in device *B*, which shows that the radiation blocking of the shadow mask is more than 99%.

The modulation frequencies between 700 Hz and 2.5 kHz lead to a mixed and complicated response behavior. This is because the response due to the crosstalk and the leaking laser beam through the shadow mask become comparable in this range. The phase and magnitude depths of the responses at above the knee frequency of the curves in Fig. 2 are associated with the interference of the responses due to the leaking laser beam and the thermal crosstalk from the source device. This is consistent with some reports on the diffraction and interference of phonons in single crystal lattices or superlattices [12], [13]. However, the detailed study of this interference in our devices requires further systematic investigation, which is beyond the scope of this paper. Here we have analyzed the crosstalk-based responses of the devices by considering them from two main aspects: 1) the effect of the separation between the devices and 2) the effect of superconductivity transition.

A. Effect of Separation Between the Devices on the Crosstalk-Based Response

The dependence of the response on the separation between the devices is shown in Fig. 2 for devices on a 1-mm-thick

TABLE I
CROSSTALK-FREE MODULATION FREQUENCIES AND THE CALCULATED DIFFUSIVITIES FOR DEVICES *A*, *C*, AND *D* AT T_{c-zero} , T_{c-mid} , AND $T_{c-onset}$

Device	d (μm)	Crosstalk-free modulation frequency (Hz)			Corresponding diffusivity (cm^2/s)*		
		T_{c-zero}	T_{c-mid}	$T_{c-onset}$	T_{c-zero}	T_{c-mid}	$T_{c-onset}$
A	40	17853	15500	-	0.030	0.028	-
C	60	7590	5850	4611	0.030	0.026	0.022
D	170	762	645	366	0.029	0.027	0.022

* Average diffusivities at T_{c-zero} , T_{c-mid} , and $T_{c-onset}$ are 0.030, 0.027, and 0.022 cm^2/s respectively.

SrTiO₃ substrate. The thermal diffusion length, that represents the characteristic penetration depth of the temperature variation into the substrate is found from [14].

$$L_f = \sqrt{\frac{D}{\pi f}} \quad (1)$$

where T_0 is the temperature at $x = 0$, f is the modulation frequency, $D = k_s/c_s$ is the thermal diffusivity of the substrate material, and k_s and c_s are the thermal conductivity and the specific heat of the substrate materials, respectively. For example, the thermal diffusion length for the SrTiO₃ substrate at 4 Hz would be 1 mm, the thickness of the substrate.

At low frequencies, all the characterized neighbor devices behaved the same, as shown in Fig. 2. That is, their response magnitude behaviors and phases are very close to each other. This is interpreted to be caused by the fact that the thermal diffusion length in this range is comparable to the substrate thickness leading to an almost similar temperature variation for all the neighbor devices. In this range of frequency, the Kapitza boundary resistance is the dominant thermal parameter affecting the response [3], [4], and all the devices behave as if they are perfectly coupled to each other. As the thermal diffusion length starts to be comparable to the distance between the devices, the response curves start to diverge from each other. Eventually, after the modulation frequency becomes high enough to cease the coupling, the devices again converge to the response of the input device *B* due to the leaking laser beam as discussed earlier. Thus, for each device at different temperatures, we can define a modulation frequency after which the crosstalk is negligible. The crosstalk-free modulation frequency values in Table I have been obtained by getting the phase minima versus modulation frequency for devices *A*, *C*, and *D*. Above these frequency values, the crosstalk is negligible and the response is only generated by the leaking input laser itself. For example, the values of the fourth column in Table I are found from the frequencies where the minimum phase occurs in the curves if Fig. 2(a).

The spatial dependence of the temperature through the substrate has already been formulated for large area bolometers assuming one-dimensional heat propagation in the vertical direction in [2], [14], [15] as given as follows:

$$T(x, t) = T_0 \exp\left[-\sqrt{\frac{\pi f}{D}}x\right] \cos\left(\omega t - \sqrt{\frac{\pi f}{D}}x\right). \quad (2)$$

We have made a finite-element modeling with ANSYS and observed that for a small area bolometer, the lateral thermal diffusion can be approximated with the same decay factor after a separation distance equal to the device width.

In the previously reported results, a clear knee frequency in the magnitude of the response versus modulation frequency curve has been observed due to the Kapitza boundary resistance at the bottom of the substrate. However, a knee frequency is not expected in the lateral direction. Thus, we calculated the diffusivity values by using (2) and the response plots. For example, the phase minimum for device *D* at T_c occurs at 645 Hz as obtained from Fig. 2(a) and the corresponding T/T_0 value is 0.009 78 as obtained from Fig. 2(b). The distance d between the device *B* and *D* is 170 μm . If we substitute the above values in (2), we get a diffusivity value of 0.027 at T_{c-mid} , as shown in Table I. According to [16] and [17], the corresponding diffusivity D for bulk SrTiO₃ is 0.12 cm^2/s . The diffusivity values found here which is derived from the basic thermal diffusion process differs from the previously reported values. This is interpreted to be due to the fact that our calculation here is mostly based on the lateral thermal conductance where [16] and [17] report the values for bulk material and for vertical thermal conductance. Hence, from an engineering point of view, one can use the diffusivity values in Table I for the calculations of the lateral thermal diffusion process for design optimizations targeting crosstalk-free operation.

B. Effect of Superconductivity Transition on the Response Behavior of the Samples

One of the immediate observations in the response of the devices is a strong temperature dependence of the phase of the source devices at low modulation frequencies f_m , as shown in Figs. 3 and 4. This has been explained for small and large area single pixel devices in [3] and [4]. There was discussed that the transition-dependent change of the phase of the response is due to the effects of the order parameter of the YBCO material on the phonon spectrum, which also determines the Kapitza boundary resistance. Since the thermal diffusion length at low modulation frequencies is greater than the device separation, the sense devices are also strongly coupled to the source device in this range of frequencies.

We have also measured the response in the illuminated device without a shadow mask to verify the above, compared to the previously reported results on the large area devices. As measured, the response of the device *B* did not change considerably compared to that of the shadowed case. We have reported the temperature-dependent response of a single device elsewhere [3], [4]. The response behavior in Fig. 3 is also affected by the gold deposition in the contact paths, the effects of which dominate the temperature dependence of the other thermal parameters in the device such as the lateral thermal conductance through the YBCO film or the film-substrate thermal resistance.

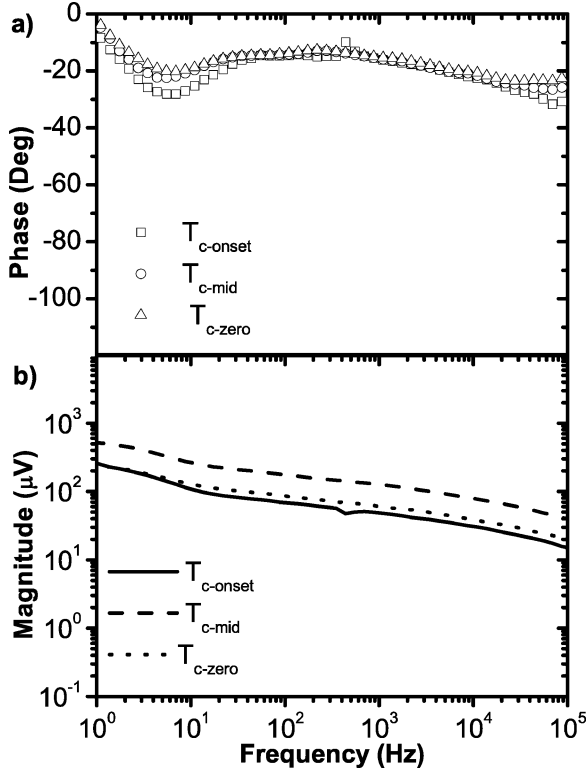


Fig. 3. (a) Phase and (b) magnitude of the IR response versus frequency of the source bolometer *B* on 1-mm-thick SrTiO₃ substrate. The data is taken at three different temperatures: T_{c-zero} , T_{c-mid} , and $T_{c-onset}$.

As shown in Fig. 3, the response of the source-device *B* does not show considerable temperature dependence. However, Figs. 4 and 5 show that the responses of devices *C* and *D* are strongly dependent on the superconductivity transition. Similar temperature-dependent results have also been obtained for device *A*. Thus, the strong temperature-dependent response of the devices *A*, *C*, and *D* are associated to be caused mainly by the superconductivity transition dependent crosstalk between the devices.

Using the phase of the response of device *D* in Fig. 4, the crosstalk-free modulation frequency at $T_{c-onset}$ is lower than that of T_{c-zero} . Based on the above, the coupling between the devices is found to be more at lower temperatures, enabling crosstalk at higher frequencies.

Using the quantitative analysis and calculation of the diffusivity values at different temperatures, as explained in Section III-A, we obtained the crosstalk-free modulation frequencies and the diffusivity values given in Table I. As observed from Table I, the diffusivity decreases as the temperature increases. The average diffusivity values were calculated to be 0.030, 0.027, and 0.022 cm²/s at T_{c-zero} , T_{c-mid} , and $T_{c-onset}$ temperatures, respectively. The increase of diffusivity as the temperature is decreased might be interpreted to be due to the change of the phonon spectrum in the YBCO film. This result agrees with the previously reported single pixel response behaviors in [3] and [4], where the phase of the response of single pixel devices also reported to increase as the temperature decreases at high modulation frequencies due to the increase of the effective thermal conductance of the devices.

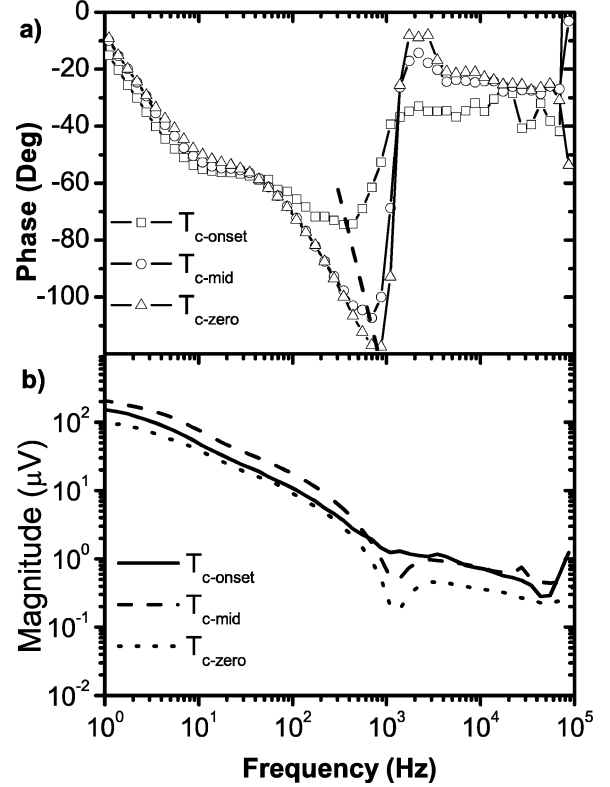


Fig. 4. (a) Phase and (b) magnitude of the IR response versus frequency of the sense bolometer *D* on 1-mm-thick SrTiO₃ substrate. The data is taken at three different temperatures: T_{c-zero} , T_{c-mid} , and $T_{c-onset}$.

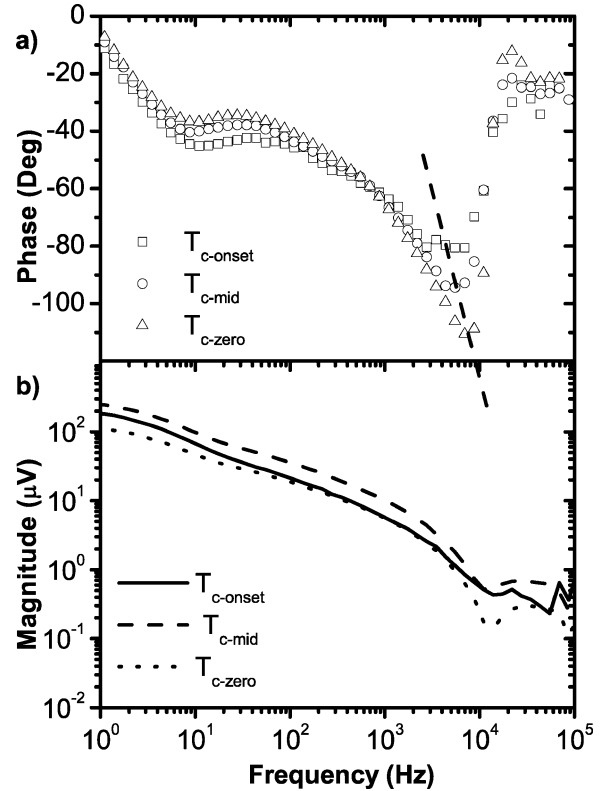


Fig. 5. (a) Phase and (b) magnitude of the IR response versus frequency of the sense bolometer *C* on 1-mm-thick SrTiO₃ substrate. The data is taken at three different temperatures: T_{c-zero} , T_{c-mid} , and $T_{c-onset}$.

IV. SUMMARY AND CONCLUSIONS

We have investigated the crosstalk between the neighbor devices in designed bolometer arrays and have shown that it is affected by the superconductivity transition, as well as the separation distance. In addition to its engineering applications, this study gives insight about the heat propagation, and the possible superconductivity transition dependent phonon mean free path in the substrates. As in the single pixel case, the superconductivity transition in our bolometer arrays is found to have a major effect on the thermal coupling between the devices and the lateral heat diffusion in the substrate. The response of the source-device does not show considerable temperature dependence, which is interpreted to be due to the dominant thermal conductance through the gold layer on the contact paths. Thus, the temperature-dependent response of the devices A , C , and D are associated to be caused mainly by the superconductivity transition dependent crosstalk between the devices. This implies that the phonon scattering and its spectrum in the substrate material should also be a function of the superconductivity parameter of the 200-nm-thin YBCO film at the transition. This is while the thickness of the engaged substrate material is orders of magnitude thicker than the YBCO film. These phenomena are also observed at relatively high temperatures of about 90 K, where the phonons' mean free paths are expected to be very short compared to the thermal diffusion length at the corresponding frequencies. The comprehensive responsible mechanism for the observed temperature dependence of the crosstalk is under further investigation.

Given the operating temperature and the device dimensions, one should use a modulation frequency greater than the crosstalk-free modulation frequency at the bias temperature for a crosstalk-free bolometer operation. This plus the consideration of the maximum signal-to-noise ratio, leads to a design optimization with the parameters of $(dR/dT)(T)$, variation of response versus modulation frequency which is application-dependent.

REFERENCES

- [1] M. Fardmanesh, "Analytic thermal modeling for DC-to-midrange modulation frequency responses of thin-film high- T_c superconductive edge-transition bolometers," *Appl. Opt.*, vol. 40, no. 7, pp. 1080–1088, Mar. 2001.
- [2] B. Dwir and D. Pavuna, "A sensitive YBaCuO thin film bolometer with ultrawide wavelength response," *J. Appl. Phys.*, vol. 72, no. 9, pp. 3855–3861, 1992.
- [3] M. Fardmanesh and I. N. Askerzade, "Temperature dependence of the phase of the response of YBCO edge-transition bolometers: Effects of superconductivity transition and thermal parameters," *Supercond. Sci. Technol.*, no. 16, pp. 28–32, 2003.
- [4] A. Bozbey, M. Fardmanesh, I. Askerzade, M. Banzet, and J. Schubert, "Effects of the superconductivity transition on the response of YBCO edge transition bolometers," *Supercond. Sci. Technol.*, vol. 16, no. 12, pp. 1554–1558, 2003.

- [5] A. Adam, A. Gauge, C. Ulysse, A. Kreisler, and C. Boulanger, "Three-temperature model for hot electron superconducting bolometers based on high- T_c superconductor for terahertz applications," *IEEE Trans. Appl. Supercond.*, pt. 1, vol. 13, no. 2, pp. 155–159, Jun. 2003.
- [6] T. May, V. Zakosarenko, R. Boucher, E. Kreysa, and E. G. Meyer, "Superconducting bolometer array with SQUID readout for submillimeter wavelength detection," *Supercond. Sci. Technol.*, vol. 16, pp. 1430–1433, 2003.
- [7] A. Gague, P. Teste, J. Delerue, A. Gensbittel, A. D. Luca, A. Kreisler, F. Voisin, G. Klisnick, and M. Redon, "YBaCuO midinfrared bolometers: substrate influence on inter-pixel crosstalk," *IEEE Trans. Appl. Supercond.*, vol. 11, no. 1, pp. 766–769, Mar. 2001.
- [8] A. V. Sergeev, A. Semenov, P. Kouminov, V. Trifonov, I. G. Goghidze, B. S. Karasik, G. N. Gol'tsman, and E. M. Gershenson, "Transparency of $\text{YBa}_2\text{Cu}_3\text{O}_{7-\delta}$ —Film/substrate interface for thermal phonons measured by means of voltage response to radiation," *Phys. Rev. B*, vol. 49, no. 13, pp. 9091–9096, Apr. 1994.
- [9] A. Litvinchuk, C. Thomsen, M. Cardona, L. Börjesson, L. Berastegui, and L.-G. Johansson, "Infrared-active phonons and the superconducting gap of T_c reduced double-chain $\text{YBa}_2\text{Cu}_4\text{O}_8$ superconductors," *Phys. Rev. B*, vol. 50, no. 2, pp. 1171–1177, 1994.
- [10] O. Misochko, E. Sherman, N. Umesaki, K. Sakai, and S. Nakashima, "Superconductivity-induced phonon anomalies in high- T_c superconductors: a Raman intensity study," *Phys. Rev. B*, vol. 59, no. 17, pp. 11 495–11 501, 1999.
- [11] O. Misochko, K. Kisoda, K. Sakai, and S. Nakashima, "Dynamics of low-frequency phonons in the $\text{YBa}_2\text{Cu}_3\text{O}_{7-x}$ superconductor studied by time- and frequency-domain spectroscopies," *Phys. Rev. B*, vol. 61, no. 6, pp. 4305–4313, 2000.
- [12] M. Giehler, T. Ruf, M. Cardona, and K. Ploog, "Interference effects in acoustic-phonon Raman scattering from GaAs/AlAs mirror-plane superlattices," *Phys. Rev. B*, vol. 55, no. 11, pp. 7124–7129, 1997.
- [13] D. Dieleman, A. Koenderink, A. Arts, and H. de Wijn, "Diffraction of coherent phonons emitted by a grating," *Phys. Rev. B*, vol. 60, no. 21, pp. 14 719–14 723, 1999.
- [14] M. Fardmanesh, *High Temperature Superconductivity 2: Engineering Applications*, A. Narlikar, Ed. New York: Springer-Verlag, 2004.
- [15] Q. Hu and P. L. Richards, "Design analysis of a high T_c superconducting microbolometer," *Appl. Phys. Lett.*, vol. 55, no. 23, pp. 2444–2446, Dec. 1998.
- [16] M. Fardmanesh, A. Rothwarf, and K. J. Scoles, "Low and midrange modulation frequency response for YBCO infrared detectors: Interface effects on the amplitude and the phase," *IEEE Trans. Appl. Supercond.*, vol. 5, no. 1, pp. 7–13, Mar. 1995.
- [17] U. P. Oppenheim, M. Katz, G. Koren, E. Polturak, and M. R. Fishman, "High temperature superconducting bolometer," *Physica C*, vol. 178, pp. 26–28, 1991.



Ali Bozbey (S'98) was born in Isparta, Turkey, on September 27, 1979. He received the B.S. and M.S. degrees in electrical and electronics engineering from Bilkent University, Turkey, in 2001 and 2003, respectively, where he is currently working toward the Ph.D. degree.

He has been a Teaching and Research Assistant at Bilkent University since 2001. He has developed an automated high-temperature superconducting bolometer characterization setup. He is currently working on the high-frequency response characteristics of bolometers and the crosstalk in the bolometer arrays. His research interests include the design and modeling of high-temperature superconducting infrared detectors in combination with SQUID-based read-out electronics. He is the author and coauthor of several journal publications.

Mr. Bozbey has been the Vice Chair of the Bilkent IEEE Student Branch at Bilkent. He has worked as one of the coordinators for the establishment of ten new IEEE student branches in Turkey.



Mehdi Fardmanesh (M'90–SM'01) was born in Tehran, Iran, in 1961 and received the B.S. degree from Tehran Polytechnic University, and the M.S. and Ph.D. degrees from Drexel University, PA, all in electrical engineering, in 1987, 1991, and 1993, respectively. In 1989, he joined the graduate program at Drexel University.

Until 1993, he conducted research in development of thin and thick film high-temperature superconducting materials and devices, as well as development of ultralow noise cryogenic characterization systems. From 1994 to 1996, he was Principal Manager for R&D and the Director of a private sector research electrophysics laboratory, while also teaching at the Departments of Electrical Engineering and Physics of Sharif University of Technology, Tehran. In 1996, he joined the Electrical and Electronics Engineering Department, Bilkent University, where he teaches in the areas of solid-state, and electronics, while supervising the Superconductivity Research Laboratory. In 1998 and 1999, he was invited to ISI-Forschungszentrum Juelich in Germany where he pursued the development of low-noise High- T_c rf-SQUID-based magnetic sensors. From 2000 to 2004, he was the international director of the Juelich-Bilkent joint project for "development of High Resolution High- T_c SQUID-based magnetic imaging system." Since 2000, he has also been with the Electrical Engineering Department of Sharif University. His research interests are focused in the areas of high-temperature superconductive bolometers, Josephson Junctions, and SQUID-based systems.

He received the Outstanding Graduate Student and Best TA awards from Drexel University. He was awarded a research fellowship by the Ben Franklin Superconductivity Center in 1989.



Juergen Schubert was born in Cologne, Germany, in 1958. He studied Physics in Cologne and received the Diploma degree in Physics in 1985. He received the Ph.D. degree from the University Köln in 1989.

He joined Research Center Jülich, Germany, in 1984. From 1985 to 1989, he developed a high-pressure sputter technique for the growth of high-temperature superconductor thin films. Since then, he is the leader of the laserlab of the ISG 1-IT of the Research Center Jülich, and he is responsible for the growth of epitaxial oxide thin films (superconducting, ferroelectric, optical transparent, conducting, etc.) using the pulsed laser deposition method. In 2002, he spent one year at Pennsylvania State University, State College, as a guest scientist in the oxide molecular beam epitaxy-group of Darrell Schlom.



Marko Banzet was born in Dinslaken, Germany, in 1973.

He joined Research Center Jülich, Germany, in 1989 as an Physics Laboratory Assistant. Since 1992, he works as a Technician in the field of superconductivity, thin-film deposition, ion beam etching, lithographic structuring, and clean room technology. Currently, he participates in vocational training as information technology engineer.